Morphometry and Floods in Small Drainage Basins Subject to Diverse Hydrogeomorphic Controls

Peter C. Patton and Victor R. Baker

Department of Geological Sciences, University of Texas at Austin, Austin, Texas 78712

Morphometric parameters such as drainage density, stream magnitude, and relief ratio are practical measures of flood potential in small (<100 mi^2) drainage basins. Stereoscopic interpretation of low-altitude aerial photographs provides the most accurate maps of basins for generating these parameters. Field surveys of a high-density limestone basin in central Texas show that 1:24,000 scale topographic maps accurately portray the efficient stream channel system but fail to reveal numerous small gullies that may form portions of hillslope hydrologic systems. Flood potential in drainage basins can be defined by a regional index computed as the standard deviations of the logarithms of the annual maximum stream-flows. High potential basins tend toward greater relief, greater drainage density, and thus greater ruggedness numbers than low–flash flood potential watersheds. For a given number of first-order channels (basin magnitude), flash flood regions have greater ruggedness numbers, indicating higher drainage densities combined with steep hillslopes and stream channel gradients. Transient controls on flood response, such as differences between local rainstorm intensities, appear to be the major influences on hydrographs in areas of moderate dissection and relief. Morphometric parameters for low-potential flash flood regions (Indiana and the Appalachian Plateau) are better estimators of frequent low-magnitude runoff events (mean annual flood), while the same parameters correlate better with the maximum flood of record in high–flood potential regions (central Texas, southern California, and north central Utah).

Introduction

The first extensive hydrologic applications of quantitative measurements of drainage basin morphology were illustrated by *Horton* [1945] and *Langbein et al.* [1947]. Horton's morphometric work has been extended by many investigators, but only a small percentage of this research has been aimed at the practical problem of relating flood hydrograph properties to permanent hydrogeomorphic controls. The basic method of relating morphometry to floods involves the identification and analysis of relationships between drainage basin characteristics, meteorological inputs, and flood hydrograph response. The most commonly employed models identify variables that are known to be significant in the processes that transform drainage basin input (high-intensity rainfall) to output (flood response). Functional relationships between various process controls and selected measures of flood response are usually established by multiple-regression analysis. A standard logarithmic expression would take the following form:

$$Q_t = aX_1bX_2cX_3d \cdots \qquad (1)$$

where

Q_t the peak discharge with return period t (or some other flood hydrograph property such as lag time);

$a, b, c, \cdots$ regression coefficients;

$X_1, X_2, \cdots$ factors controlling the flood response.

In practice this approach has resulted in many 'flood formulas,' nearly all of which include basin area as one of the variables. Unfortunately, the approach usually involves many parameters that are dependent in some way on one another. Identifying and quantifying individual factors poses a major difficulty in the establishment of meaningful statistical relationships between various controls.

The purpose of this study is to compare and contrast morphometric properties of small (<100 mi^2) drainage basins in regions of high flood potential with drainage basin parameters

from regions of low flood potential. Basins were selected on the basis of hydrologic studies by *Beard* [1975], which defined flood potential as the standard deviation of the logarithms of the annual maximum streamflows. Because a proper understanding of the correlations derived in this study requires an appreciation of methodological limitations, this report will also consider the following: (1) the selection of parameters related to flood potential that can be measured from topographic maps or remote sensing imagery, (2) the resolution capabilities of the various sources of morphometric variables, and (3) the distinction between transient and permanent controls [*Rodda*, 1969] on local flood response characteristics.

Morphometric Parameters Useful in Estimating Flood Response

Drainage area is perhaps the most frequently employed variable in the estimation of stream discharge. Area has been correlated both with frequent runoff events of low magnitude [*Hack*, 1957] and with infrequent runoff events of high magnitude [*Patton and Baker*, 1975]; it has been used with runoff in humid [*Benson*, 1962] and arid [*Burkham*, 1966] regions. *Gray* [1970] reviewed numerous examples for regions throughout the world. In the present study, drainage areas were determined from U.S. Geological Survey water supply papers or, when necessary, by measurement from topographic maps with a polar planimeter.

Horton [1932, 1945] suggested that, in addition to area, stream slope and drainage density should be highly correlated with maximum flood discharge. Drainage density, the length of the channel per unit of drainage area, is controlled by numerous variables, including the relief, rainfall, infiltration capacity of the terrain, and resistance of the land to erosion [*Horton*, 1945]. Drainage density has been correlated with measures of relief and relief ratio [*Schumm*, 1956; *Hadley and Schumm*, 1961], the Thornthwaites precipitation effectiveness index and the runoff intensity [*Melton*, 1957], the intensity of precipitation [*Chorley*, 1957], the infiltration capacity [*Hadley and Schumm*, 1961], stream base flow [*Carlston*, 1963; *Trainer*, 1969], and the mean annual flood [*Carlston*, 1963; *Hadley and*

Schumm, 1961]. Because of the interactions between process and form variables summarized by the drainage density measure [*Horton,* 1945; *Strahler,* 1958] and because of the wide range of naturally occurring values of drainage density [*Schumm,* 1956] it is an important variable. Certainly, in a very simplistic view, drainage density measures basin efficiency in removing excess precipitation inputs.

In an analysis of flood potential one might expect flood prone regions to be characterized by high drainage density values indicating low infiltration capacity, relatively short steep slopes, and low vegetative cover, all of which would lead to the rapid concentration of flood runoff. Low-flood potential regions might be expected to have low drainage density values, reflecting the inverse of the above conditions. The erodibility of the terrain, a function of local geology or relict drainage systems that result from paleoclimates, can add considerable complexity to this generalization.

A technical problem with the use of drainage density is the difficulty of measurement, particularly when large basins are considered. This problem can be circumvented by employing the line intersection–estimating procedure. First introduced by *Carlston and Langbein* [1960] and later modified by *McCoy* [1971] and *Mark* [1974], the technique involves superimposing a grid over the drainage net and counting the number of intersections of drainage lines along a traverse line. Drainage density can then be calculated from several empirical equations employing the quotient of the number of intersections (N) and the traverse length (L):

$$DD = 1.414N/L \qquad (2)$$

from *Carlston and Langbein* [1960]

$$DD = 1.8 + 1.27N/L \qquad (3)$$

from *McCoy* [1971]

$$DD = 1.571N/L \qquad (4)$$

from *Mark* [1974].

This technique was used for calculating drainage density for six basins in north central Utah. For comparison, drainage density for the six basins was also calculated by measuring the total stream length and dividing by drainage area. Equation (3) gave the best results, showing less than 10% error (Table 1). Considering the rapidity of the technique the error was acceptable.

Stream order has been directly correlated with discharge by numerous workers [*Blyth and Rodda,* 1973; *Rodda,* 1969; *Stall and Fok,* 1967]. *Stall and Fok* [1967] noted an increasing

goodness of fit between discharge and stream order with decreasing frequency of the runoff event. This suggested that higher-magnitude events are most important in the establishment of the drainage network. *Shreve's* [1967] method of ordering has been advocated by a number of investigators as being more descriptive of network form in relation to streamflow. The number of first-order streams (Shreve magnitude) has been correlated with the peak discharge of Appalachian streams [*Morisawa,* 1962] and central Texas streams [*Patton and Baker,* 1975]. In addition, *Blyth and Rodda* [1973] noted that the number of flowing first-order streams increased with total rainfall and rainfall intensity. They noted that during dry periods, flowing first-order streams constituted less than 20% of the total flowing length of the network. At the maximum extent of the network the total length of first-order streams constituted over 50% of the total basin stream length.

The importance of basin relief as a hydrologic parameter has been noted by numerous investigators [*Sherman,* 1932; *Horton,* 1945; *Strahler,* 1958]. With increasing relief, steeper hillslopes, and higher stream gradients, time of concentration of runoff increases, thereby increasing flood peaks. Thus all other conditions being equal, the greater the relief of a basin, the greater the rate of hydrograph rise. In order to compare relief among basins of varying sizes, two dimensionless parameters were calculated. Relief ratio [*Schumm,* 1956] is the ratio of basin relief to basin length. Basin relief is measured by averaging the elevation of the divide and subtracting the elevation of the outlet. Basin length is measured parallel to the main stream. Ruggedness number [*Melton,* 1957] is the dimensionless product of drainage density and relief; and therefore areas of high drainage density and low relief are as rugged as areas of low drainage density and high relief. Areas of potential flash flooding might be expected to have the highest ruggedness numbers incorporating a fine drainage texture, with minimal length of overland flow across steep slopes, and high stream channel gradients. The combination of these factors might result in far higher flood peaks for an equivalent rainfall input than for basins having a low ruggedness number.

THE PROBLEM OF NETWORK RESOLUTION

Leopold and Langbein [1963] noted that in geomorphic systems the ability to measure may always exceed any ability to forecast. Although the present study is concerned with aspects of the network geometry that have adjusted to climatic and geologic factors, only a portion of a drainage form of a network can be attributed to these deterministic factors. The rest has been ascribed to topological randomness [*Shreve,* 1966,

TABLE 1. Drainage Density Values for Basins in North Central Utah According to Various Calculation Procedures

Basin	N/L*	1.571N/L*†	1.414N/L*‡	Measured Drainage Density, mi/mi²
City Creek	6.04	9.49	8.54	8.87
Centerville Canyon	4.72	7.50	6.65	6.67
Farmington Canyon	5.37	8.44	7.60	7.47
Ricks Creek	4.93	7.74	6.97	7.50
Parrish Creek	4.72	7.44	6.68	7.36
Holmes Creek	6.53	10.26	9.23	8.96

The coefficients derived by regression analysis for these basins are $DD = 1.442N/L$, $R^2 = 0.9979$, and $P < 0.0001$.

*N/L is the number of intersections per traverse length in miles.
†For the coefficient 1.571, error ranges from 1.1 to 13%.
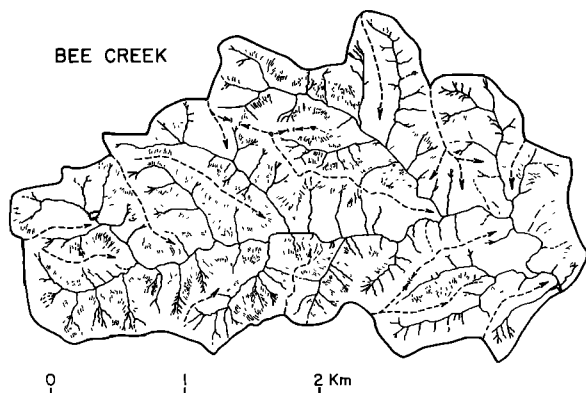‡For the coefficient 1.414, error ranges from 0.3 to 9.2%.

Fig. 1. Drainage map of Bee Creek basin near Austin, Texas, constructed by detailed stereoscopic interpretation of panchromatic aerial photographs at a 1:13,000 scale.

1967; *Smart*, 1969]. Whatever the purpose of the investigation, however, the detailed mapping of the drainage network is the initial step in quantitative drainage basin studies. The most precise data, of course, comes from field determinations. Because this method is slow and often costly, standard topographic maps have become a favorite source of data.

In order to compare the resolution capabilities of various scales and types of drainage network data sources, a number of detailed studies were completed on Bee Creek, a small tributary of the Colorado River, near Austin, Texas. The hydrology of Bee Creek was described by *Tinkler* [1971]. The basin is developed on deeply dissected marl and limestone bedrock. It is characterized by steep slopes, brushy vegetation, thin soils, and a high relief ratio (0.03).

The most detailed network analysis of Bee Creek (3.4 mi^2) utilized low-altitude black and white aerial photographs at a 1:13,000 scale (Figure 1). Photographic mapping on stereo pairs was used to interpret the most subtle changes in shadow that could be interpreted as a stream channel. Besides the continuous channel network, many small discontinuous gullies which develop on the slopes of Bee Creek were easily interpreted from the stereo pairs. This technique resolved 316 unbranched tributaries (first-order segments or first-magnitude links) in the continuous network exclusive of the hill slope gully system. The total number of first-order collectors, discontinuous gullies plus first-order segments, was 995.

An additional mapping source was the Austin west quadrangle, with a 1:24,000 scale and a 20-ft contour interval (Figure 2). The drainage network composition interpreted from the topographic map (Figure 3) was less detailed than that revealed by the low-altitude stereomapping. Only 109 first-order streams were resolved.

An absolute basis of resolution capability for Bee Creek was established by detailed field surveys for selected subbasins (Figure 2). The features which acted as first-order stream segments in the field were found to be precisely those segments mapped as discontinuous gullies in the detailed stereoscopic interpretation of low-altitude black and white aerial photographs. The gullies were found to average less than 100 ft in length and were characterized by broad shallow channels cut in rock (Figure 4). The frequency of first-order gullies in the selected subbasins was 290 per square mile. The extrapolated number of 986 gullies over the entire basin compares remarkably well with the number estimated by detailed stereoscopic interpretation of the aerial photographs.

A number of studies similar to the one discussed above have
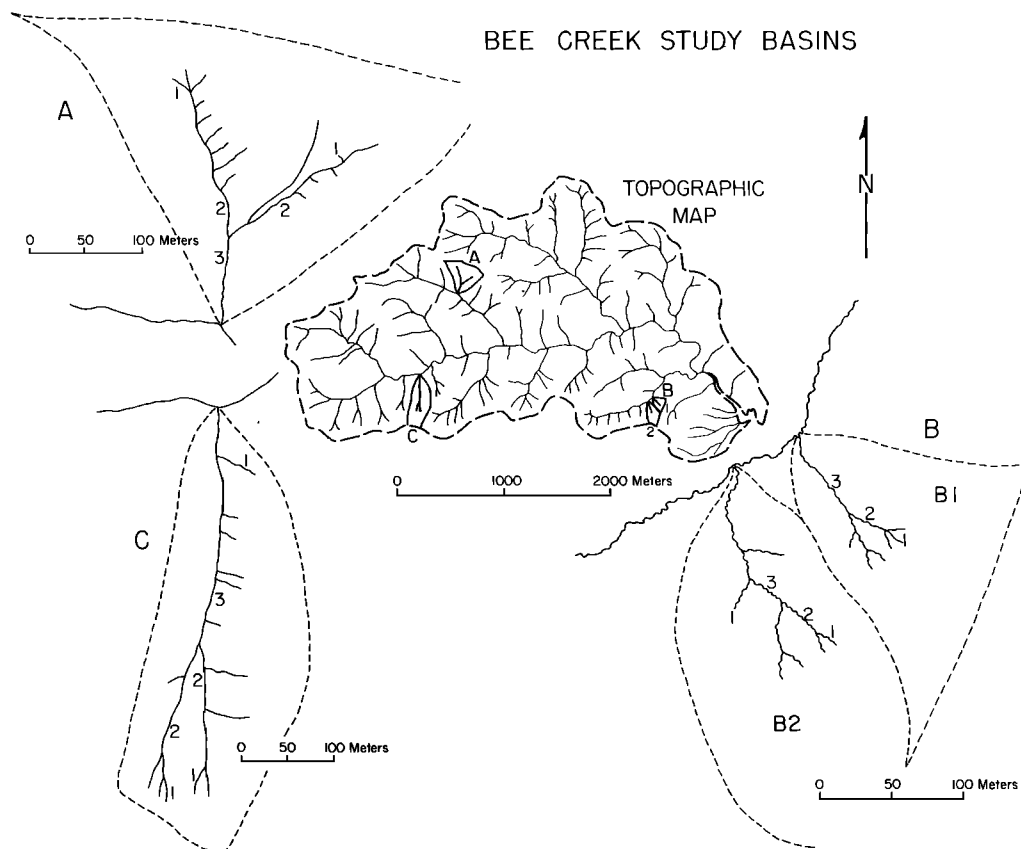

Fig. 2. Drainage map of Bee Creek constructed by the 'method of V's,' using the Austin west 7.5' topographic quadrangle map (1 : 24,000 scale). Subbasins A, B, and C were mapped by detailed field survey with compass and tape.

been done for basins in central Texas [*Baker et al.*, 1975]. In general, high relief gullied basins are not resolved adequately by 1:24,000 scale topographic maps, while low-relief basins show very little difference between field surveys, topographic maps, and detailed stereoscopic interpretations of low-altitude aerial photography. In the high-relief basins the hydrologic significance of the gullies is certainly much less than that of the continuous channel network. The gullies probably constitute a rill component of the hill slope hydrologic systems. Their high channel roughness and irregular gradients clearly distinguish them from the more efficient channel system shown on the topographic map. Purely as a practical expedient for regional comparisons, large-scale topographic maps were utilized for the streamflow estimates in the present study. Clearly, however, the accuracy of such maps for predicting flood response from diverse terrains needs to be tested in future research.

SELECTION OF STUDY BASINS

Hydrologically diverse areas in which to examine morphometric models of flood response were established by employing several measures of regional flood potential. Two of the measures were developed by *Beard* [1975]. The first is the flash flood magnitude index, which equals $[\Sigma X^2/(N - 1)]^{1/2}$, where X is the deviation of an annual maximum streamflow from the mean (expressed as a logarithm) and N is the number of events in the record. The second measure is the flash flood warning index, which equals Q_{max}/Q_{3m}, where Q_{max} is the annual maximum peak flow and Q_{3m} is the average rate of flow for a 3-day period prior to and including the day of occurrence of the peak flow.

The flash flood magnitude index is an estimator of the ratio of rare flood events to common flood events as they would be represented on a plot of discharge versus exceedence frequency per 100 events in a standard log Pearson type 3 frequency analysis [*Beard,* 1975]. *Beard* [1975] applied this criterion in
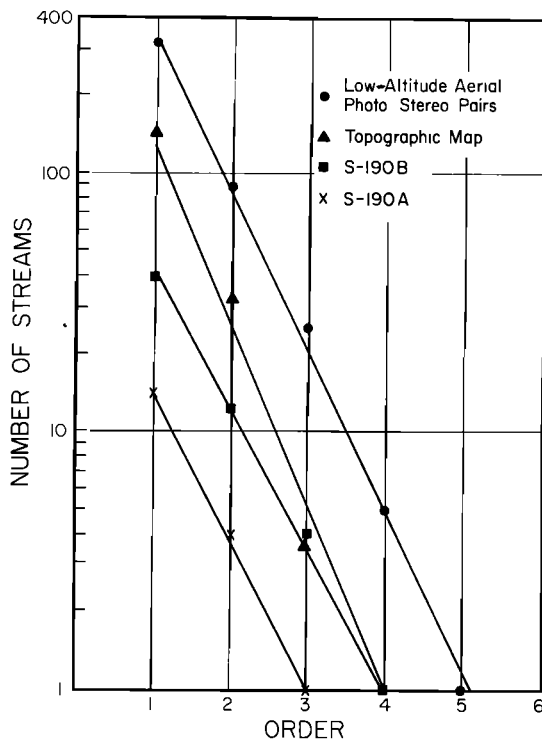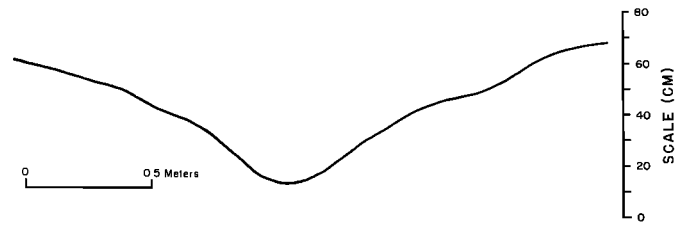

Fig. 4.   Measured cross section of a first-order gully in the Bee Creek drainage basin.

the analysis of unregulated flow records from 2900 streamflow stations in the United States under 1000 mi² in area and with record lengths equal to or exceeding 20 years.

The flash flood warning index was developed as a regional measure of the rate of rise of streamflow. The complete daily records of 260 stations were analyzed and regionalized over the entire United States to represent warning times for 1-mi² drainage areas [*Beard,* 1975]. This index was used in this study as a general guide for locating regions subject to flash floods.

The flash flood magnitude index map of the United States (Figure 5) developed by *Beard* [1975] allowed a ready means of distinguishing high- from low–flood potential regions. The study areas selected to represent high flash flood potential were central Texas, the Wasatch Mountains in north central Utah, and the San Gabriel Mountains in southern California. The regions of low potential selected are Indiana and the Appalachian Plateau province in western Pennsylvania, Maryland, Ohio, West Virginia, and Tennessee.

Flood prone areas were also designated by their historic tendency to experience flash floods. A flash flood is variously defined as (1) a sudden flood in a usually dry valley, resulting from a cloudburst [*American Geological Institute,* 1972], or (2) a local flood of great volume and short duration, generally resulting from heavy rainfall in the immediate vicinity [*Webster,* 1965]. The hydrologic implications of these vague definitions are that (1) the rate of rise of the flood hydrograph is extremely rapid and (2) because of the intensity of rainfall required for the generation of a flash flood the drainage area affected is relatively small. In his description of flash floods along the Wasatch Mountains in Utah, *Woolley* [1946] included hydrographs for Price River (drainage area of 530 mi²) and San Rafael River (drainage area of 1690 mi²) which demonstrated the rapid rise of flood stage as a result of cloudbursts. However, these rapid rises were probably a result of runoff from only a few much smaller tributaries. Similarly, in central Texas, rapid runoff from Bleiders Creek (drainage area of 16 mi²) on May 11 and 12, 1972, as a result of 16 in. of rain concentrated in 4 hours caused a rapid rise on the Comal River hours before the runoff from the dry Comal River basin peaked (Figure 6). Furthermore, flash floods may produce record discharges on small streams even though the runoff in the major drainages may be of a far lower recurrence interval. For these reasons the study was restricted to basins less than 100 mi² in area.

Where it was possible, published morphometric data were used to generate predictive equations. However, for two regions, central Texas and north central Utah, data were specifically generated for this study by topographic map analysis. The drainage network was interpreted from 1:24,000 scale maps using *Strahler's* [1957] crenulation method. The stream network was ordered by the *Strahler* [1957] and the *Shreve* [1966] method. Areal measurements were made with a polar planimeter, and linear measurements were made with a map wheel.

Fig. 3.   *Horton's* [1945] law of stream numbers as interpreted from various depictions of the Bee Creek drainage network.
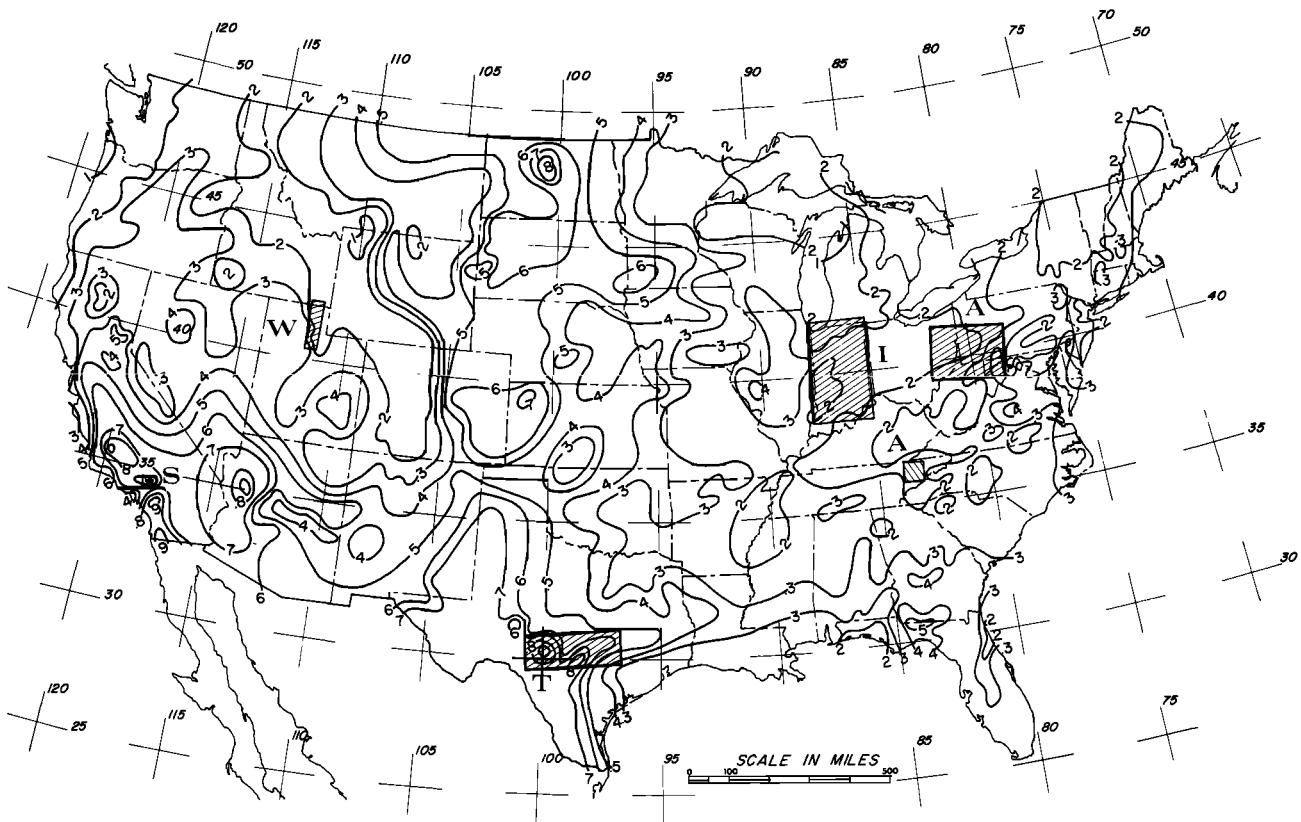
Fig. 5. Location of study areas in relation to the regional variation in the flash flood magnitude index for the United States (simplified from *Beard* [1975]). The symbols are T, central Texas; W, Wasatch front; S, southern California; I, Indiana; and A, the Appalachian Plateau.

Stream discharge records were gathered from published U.S. Geological Survey records and U.S. Forest Service open file reports. The log Pearson 3 frequency analysis was used to calculate exceedence probabilities from the annual peak data [*Beard*, 1974]. Where discharge data were not available, regional runoff equations were employed [*Patton and Baker*, 1975]. Morphometric and discharge data were reduced and analyzed by standard statistical techniques, including correlation, discriminant function, and multiple-regression methods [*Krumbein and Graybill*, 1965; *Snedecor and Cochran*, 1967]. To avoid spurious correlations between morphometric variables and discharge, drainage area and those variables highly correlated with area (e.g., basin length) were eliminated from the analysis of stream runoff.

FLOOD RESPONSE IN DIVERSE HYDROGEOMORPHIC TERRAINS

Central Texas. Central Texas has perhaps the most catastrophic rainfall-runoff regime in the conterminous United States. Texas rainfalls between 1- and 24-hour duration approach the world maxima [*Baker*, 1975]. In addition, it is one of the two regions in the United States which have the highest 10-year flood magnitudes for 300-mi² drainage basins [*Leopold et al.*, 1964]. Flooding is often the result of intense thunderstorms, and therefore the spatial and temporal distribution of flooding is extremely unpredictable.

Morphometric data were collected for 13 study basins throughout central Texas (Table 2). The drainage basins were located in diverse physiographic regions on a variety of rock types. Basins are located on the Precambrian metamorphic and igneous rocks of the Llano uplift, on the Paleozoic limestone units in north central Texas, on the Cretaceous limestone of the Edwards Plateau, and on the Cretaceous and younger

sediments of the Gulf Coastal Plain. This diversity results in a wide range of drainage basin morphometric characteristics. Relief, measured as relief ratio, is highly variable, ranging from low values on the Gulf Coastal Plain (0.010) and in north central Texas (0.007) to higher values in the Llano region (0.020) and on the Edwards Plateau (0.030). The same trend is

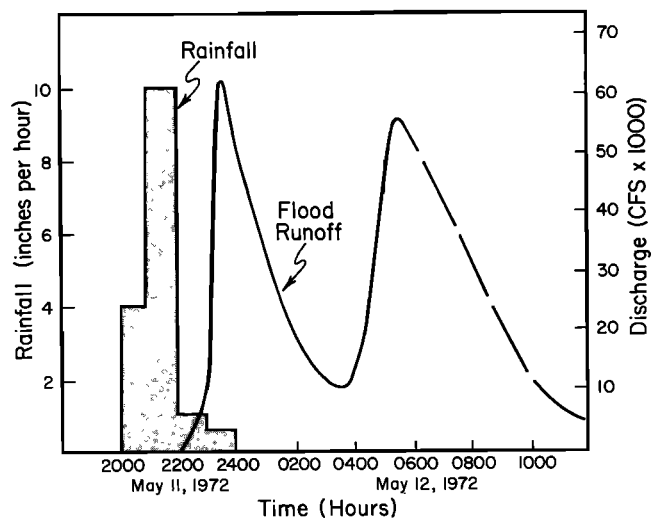Fig. 6. Rainfall and runoff for Comal River at New Braunfels, Texas, flood of May 11–12, 1972. Rainfall distribution assumes that the 16-in. recorded maximum was time distributed according to a unit distribution of storm rainfall recorded at Canyon Dam [*Colwick et al.*, 1973]. Runoff was computed by the U.S. Geological Survey from visual observations of water surface elevations at regular time intervals.

TABLE 2. Morphometric and Runoff Data for Central Texas

Basin	A, mi^2	S	M	R, ft	BL, mi	HD	RR	DD, mi/mi^2	F_1, no./mi^2	Q_{max}, ft^3/s
Deep Creek 3	3.42	4	42	270	2.77	0.23	0.018	4.37	12.28	3060
Deep Creek 8	5.41	3	44	270	3.86	0.17	0.013	3.30	8.13	5660
Wilbarger Creek	4.61	3	24	165	3.05	0.10	0.010	3.24	5.20	4279
Rebecca Creek	11.41	6	237	512	4.36	0.61	0.022	6.14	21.27	9300
Dry Creek (Buescher L.)	1.57	4	84	142	1.94	0.27	0.014	10.26	53.50	1870
Mukewater 9	4.02	4	91	135	3.61	0.15	0.007	5.66	22.64	1440
Upshaw Creek	4.89	5	105	340	3.72	0.41	0.017	6.20	21.47	4460*
Helms Creek	5.92	5	147	505	4.64	0.66	0.021	7.01	24.83	5120*
Dry Creek	1.79	4	81	375	1.68	0.64	0.040	8.90	45.25	2145*
Burleson Creek	4.16	5	90	437	3.39	0.52	0.024	6.51	21.63	3985*
Little Barton Creek	5.95	5	101	442	4.69	0.44	0.018	5.24	16.97	5150*
Miller Creek	5.71	6	291	661	3.43	1.19	0.036	9.68	50.96	5010*
Bee Creek	3.43	4	145	540	3.34	0.81	0.030	8.10	42.27	3395*

Symbols are as follows: A, drainage basin area; S, Strahler basin order; M, basin magnitude; R, basin relief; BL, basin length; HD, ruggedness number; RR, relief ratio; DD, drainage density; F_1, first-order channel frequency; and Q_{max}, maximum peak discharge.
*Estimated from regional runoff equation $Q_{max} = 1403A^{0.73}$ [Patton and Baker, 1975].

followed by values of drainage density, first-order stream frequency, and ruggedness number.

The Wasatch front. Woolley [1946] noted that in north central Utah between 1847 and 1938 over 500 cloudburst floods were recorded along with reports of extensive crop damage and highway, bridge, and building destruction. Butler and Marsell [1972] detail the 836 flash floods reported between 1939 and 1969, the majority of which occurred along the Wasatch front. These floods are the result of intense rainfalls, up to 4 in. in 12 hours, from severe thunderstorms created by the orographic effect of the Wasatch front [Butler and Marsell, 1972]. Although the volume of flood runoff is considerably less here than for central Texas, flash floods commonly cause mud and debris flows which greatly increase property damage [Woolley, 1946]. Interestingly, the flash flood magnitude index for this region is extremely low, ranging from 1.5 to 3.5. This is because the magnitude index is calculated from the distribution of the annual peak flows, which along the Wasatch front are related to snowmelt events (see U.S. Geological Survey Water-Supply Paper 1927).

Eleven drainage basins along the Wasatch front were selected for study (Table 3). The drainages investigated have their headwaters east of the Wasatch fault and flow westward, eroding steep canyons into the fault scarp. Where the streams exit from the mountain front, broad alluvial fans have formed on top of Pleistocene lacustrine sediments. Most of the small

drainage basins are underlain by the Precambrian Farmington Canyon complex composed of metamorphic sedimentary rocks, metamorphic igneous rocks, and intrusive gneiss [Eardley, 1944]. The larger basins are eroding into the Triassic clastic sediments and, in places, cross narrow belts of Paleozoic clastic and carbonate rocks [Eardley, 1944]. In general, the drainage basins have high relief (relief ratio, 0.08–0.27), high drainage density (6.68–10.01 mi/mi^2) and extremely high ruggedness numbers (4.60–10.95).

Southern California. Intense precipitation in southern California is controlled by extratropical North Pacific cyclones which move inland, generating storms with recorded intensities of up to 11.5 in. in 1 h 20 m [Anderson, 1949]. The mountainous regions of southern California are particularly affected by flash flooding, runoff being up to 1260 ft^3/s/mi^2 from a 17-mi^2 drainage basin [Anderson, 1949]. Therefore the San Dimas experimental forest on the southern slope of the San Gabriel Mountains near Los Angeles was an excellent locality for analysis. The regional flash flood magnitude index is 0.7. Runoff in the San Dimas region is locally even more erratic, the flash flood magnitude index approaching or exceeding 1.0 for many basins.

The San Gabriel Mountains are a fault block range bounded by three major fault zones [Maxwell, 1960]. The mountains themselves are highly faulted and consist of pre-Cretaceous schist, gneiss and granitic rocks surrounded by Tertiary and

TABLE 3. Morphometric and Runoff Data for North Central Utah

Basin	A, mi^2	S	M	R, ft	BL, mi	HD	RR	DD, mi/mi^2	F_1, no./mi^2	$Q_{0.5}$, ft^3/s	$Q_{0.1}$, ft^3/s	$Q_{0.01}$, ft^3/s	Q_{max}, ft^3/s
City Creek	19.2	5	602	4150	10.23	6.71	0.080	8.54	31.35	64	109	167	163
Hardscrabble Creek	28.10	5	1028	3230	7.65	4.84	0.080	8.02	36.58	252	416	638	464
Centerville Canyon	3.15	4	71	3600	3.77	4.60	0.180	6.75	22.54	12	28	62	30
Farmington Canyon	10.60	5	276	3170	6.29	4.56	0.095	7.60	26.03	142	300	598	298
Emigration Creek	18.00	5	629	3575	8.33	5.72	0.081	8.65	34.94	25	63	137	156
Mill Creek (Salt Lake City)	21.70	5	785	4540	9.65	7.26	0.089	8.61	36.17	50	91	151	152
Rick Creek	2.35	4	68	4300	3.04	5.67	0.270	6.97	28.94	17	48	130	51
Parrish Creek	2.08	3	55	4255	3.63	5.10	0.220	6.68	26.44	12	31	72	30
Holmes Creek	2.49	4	98	4100	2.84	7.17	0.270	9.23	39.35	17	39	85	36
Dry Creek	9.82	6	354	5785	5.27	10.95	0.210	10.01	36.04	210	385	682	597
Mill Creek (Bountiful)	8.79	5	307	3945	6.07	6.08	0.120	8.15	34.92	40	103	248	140

Symbols are the same as those defined in Table 2 with the addition of $Q_{0.5}$, discharge with 0.5 exceedence probability per 100 events; $Q_{0.1}$, discharge with 0.1 exceedence probability per 100 events; and $Q_{0.01}$, discharge with 0.01 exceedence probability per 100 events.

TABLE 4. Morphometric and Runoff Data for San Dimas Experimental Forest, Southern California

Basin	A, mi^2	S	M	R, ft	BL, mi	HD	RR	DD, mi/mi^2	F_1, no./mi^2	$Q_{0.5}$, ft^3/s	$Q_{0.1}$, ft^3/s	$Q_{0.01}$, ft^3/s	Q_{max}, ft^3/s
Wolfskill Canyon Watershed 1	2.49	5	409	2695	2.56	9.83	0.199	19.26	164.25	24	202	1311	1010
Fern Canyon Watershed 2	2.20	5	465	2900	2.46	10.16	0.223	18.50	211.36	19	149	1040	215
Upper East Fork Watershed 3	2.18	5	347	2560	2.56	8.63	0.189	17.81	159.17	13	118	905	160
Bell Canyon Watershed 8	2.01	5	386	1520	2.21	7.02	0.130	24.40	192.03	15	165	1710	217
Wolfe Canyon Watershed 9	1.18	5	344	1610	1.86	7.59	0.163	24.91	291.52	2	83	1862	145
Subwatershed 2-1	0.054	3	19	727	0.41	2.51	0.337	18.27	351.85	1	11	95	22
Subwatershed 2-2	0.065	3	22	647	0.48	2.28	0.252	18.61	338.46	2	20	190	22
Subwatershed 2-3	0.085	2	13	990	0.55	2.53	0.337	13.50	152.94	1	19	233	51
Subwatershed 8-1	0.122	4	55	992	0.68	5.52	0.277	29.38	450.81	0.5	14	827	22
Subwatershed 8-2	0.061	5	75	719	0.38	4.48	0.360	32.94	1229.5	0.7	26	862	33
Subwatershed 8-3	0.10	4	39	1031	0.54	5.62	0.358	28.81	390.0	0.6	10	150	18
Subwatershed 8-4	0.061	3	13	921	0.45	3.14	0.390	18.02	213.1	0.4	8	139	10

Symbols are the same as those defined in Tables 2 and 3.
Morphometric data are from *Maxwell* [1960].

Quaternary alluvial deposits [*Maxwell*, 1960]. Morphometric data measured by *Maxwell* [1960] were used from 12 basins (Table 4) within the San Dimas experimental forest. Relief is high (relief ratio, 0.130–0.390), and drainage density is extremely high (13.50–32.94 mi/mi^2). As a result, the ruggedness number is high again (1.85–10.16), indicating extremely high relief fine-textured drainage basins. The fine texture of the drainage network is demonstrated by the frequency of first-order streams which exceed 3600 per square mile in one basin. This demonstrates that as drainage density increases, the increase in total channel length is created as the result of a far greater increase in first-order streams and not as the result of an increase in the length of higher-order channels.

Indiana. Regional and at-station flash flood magnitude indices for Indiana are quite low, ranging from 0.2 to 0.3. In this area of relatively low flood potential, 10 basins [*Lee and Del-leur*, 1972] were selected for study (Table 5). With the exception of south central Indiana, the entire state is covered by a thickness of more than 50 ft of glacial ground and end moraine (data from Indiana State Geological Survey regional maps 1–8). Of the basins investigated, only one crosses significant outcrops of Mississippian shale, siltstone, and sandstone; the others are underlain by Wisconsinan and Illinoisan glacial material (data from Indiana State Geological Survey regional maps 1–8). Basin relief is extremely low in Indiana (relief ratio, 0.0008–0.016), but drainage densities (2.17–11.80 mi/mi^2) can

be as high as values in the Wasatch front and are generally comparable to values for central Texas. This can in part be attributed to the easily eroded impermeable till underlying most of the drainage basins (data from Indiana State Geological Survey regional maps 1–8). The ruggedness number is slightly lower for Indiana than for the previously discussed regions of high flash flood potential.

The Appalachian Plateau. Eleven basins (Table 6) were chosen for study within the Allegheny Mountain, unglaciated Allegheny Plateau, and Cumberland Plateau divisions of the Appalachian Plateau [*Morisawa*, 1962]. The region contains Paleozoic rocks, gently folded in the Allegheny Mountain region, becoming more horizontal westward and southward onto the unglaciated Allegheny Plateau and the Cumberland Plateau. In this region, basin relief ranges from low to intermediate values (relief ratio, 0.005–0.067), but drainage density is consistently low (2.58–5.75 mi/mi^2), and as a result, ruggedness numbers have intermediate values (0.17–1.11). The low drainage density values in basins with intermediate relief probably indicate the greater infiltration capacity of thicker soils and the increased vegetative cover prohibiting erosion. For example, several Texas streams have lower values of relief ratio but greater values of drainage density. Ruggedness numbers, however, are nearly identical for the two regions.

Correlation analysis. Morphometric data from each of the five study regions were compared (1) to stream discharge

TABLE 5. Morphometric and Runoff Data for Indiana

Basin	A, mi^2	S	M	R	BL, mi	HD	RR	DD, mi/mi^2	F_1, no./mi^2	$Q_{0.5}$, ft^3/s	$Q_{0.1}$, ft^3/s	$Q_{0.01}$, ft^3/s	Q_{max}, ft^3/s
Little Indian Creek	33.43	6	129	77	8.82	0.031	0.0016	2.17	3.85	343	500	726	500
Lawrence Creek	.2.64	4	97	120	2.17	0.139	0.010	6.10	36.74	527	1350	3,247	2,650
Bear Creek	5.80	5	259	310	3.66	0.575	0.016	9.80	44.65	603	1573	3,792	1,830
Bean Blossom Creek	13.40	6	785	373	5.22	0.833	0.013	11.80	58.58	1792	4651	11,108	8,140
Big Blue River	169.70	6	3066	240	26.39	0.222	0.0017	4.88	18.07	4265	8807	17,006	12,900
Hinkle Creek	18.20	6	624	110	4.83	0.138	0.0043	6.62	34.28	1346	4206	12,291	4,920
Cicero Creek	205.7	7	3066	200	18.40	0.163	0.0020	4.30	14.90	3311	7548	15,942	9,800
Buck Creek	33.84	6	817	45	9.72	0.048	0.0008	5.69	24.14	810	1792	3,760	1,780
Salamonie River	80.55	7	2159	182	12.03	0.200	0.0028	5.82	26.80	2155	3803	6,686	3,460
Little Cicero Creek	42.06	6	1003	110	9.68	0.096	0.0021	4.64	23.85	1242	2960	6,701	3,980

Symbols are the same as those defined in Tables 2 and 3.
Morphometric data are from *Lee and Delleur* [1972].

TABLE 6. Morphometric and Runoff Data for the Appalachian Plateau

Basin	A, mi^2	S	M	R	BL, mi	HD	RR	DD, mi/mi^2	F_1, no./mi^2	$Q_{0.5}$, ft^3/s	$Q_{0.1}$, ft^3/s	$Q_{0.01}$, ft^3/s	Q_{max}, ft^3/s
Tar Hollow Creek	1.5	4	74	330	3.2	0.17	0.048	2.79	49.33	127	337	803	957
Home Creek	1.6	5	70	210	3.4	0.23	0.035	5.75	43.75	123	293	618	378
Mill Creek	2.7	4	104	400	4.3	0.44	0.030	5.66	38.52				
Green Lick Run	3.1	4	79	860	2.2	0.59	0.067	3.65	25.48	263	607	1,244	1,400
Beech Creek	18.7	5	186	550	14.8	0.29	0.007	2.84	9.95	1062	2,083	4,124	2,210
Piney Creek	24.5	5	271	1650	14.9	0.95	0.021	3.04	11.06	1093	2,685	5,834	6,850
Casselman River	62.5	6	653	1700	25.1	1.07	0.013	3.34	10.45	2320	4,442	8,034	8,400
Emory River	83.2	7	1936	540	25.8	0.57	0.004	5.57	23.27	7233	13,759	24,095	18,700
Youghlogheny River	134.0	6	1798	1590	25.1	1.11	0.012	3.68	13.41	4375	8,535	15,447	11,800
Daddys Creek	93.5	6	1181	730	27.8	0.40	0.005	2.87	12.63	4612	9,346	17,430	11,600
Little Mahoning Creek	87.4	6	1058	1500	25.8	0.73	0.011	2.58	12.10	3059	5,056	7,849	5,300
Allegheny River	55.0	7	5966	1010	27.4	0.56	0.007	2.92	10.84	7562	5,708	29,182	55,000

Symbols are the same as those defined in Tables 2 and 3.
Morphometric data are from *Morisawa* [1962].

values having an exceedence probability per 100 events of 0.1, 0.5, and 0.01 and (2) to the maximum discharge of record. For the central Texas watersheds it was feasible to include only the maximum discharge of record. The correlation matrices are presented in Tables 7, 8, 9, 10, and 11.

Basin magnitude, the total number of first-order streams, correlates best with infrequent runoff events in the San Dimas and Wasatch watersheds, whereas in the Indiana and Appalachian Plateau watersheds the correlation coefficients between basin magnitude and discharge increase with increasing frequency of runoff. This suggests that regions characterized by infrequent high-intensity storms adjust their drainage net to the infrequent high-magnitude runoff events. Regions characterized by more frequent less intense regional storms adjust their drainage nets to the resulting more frequent lower-magnitude floods such as the mean annual flood. The result is not completely independent of drainage area, as is shown by the high correlation of area to basin magnitude in several regions. Basin magnitude was used in the regression analysis because recent studies have shown that it is a more sensitive measure of drainage basin response than is area [*Blyth and Rodda*, 1973].

Flood formulas. Equations were developed for flood prediction in each of the five regions by stepwise least squares regression statistics (Table 12). Basin magnitude was employed along with drainage density, first-order stream frequency, relief ratio, and ruggedness number. Drainage density was not employed in the equations with first-order stream frequency, as they are highly correlated [*Melton*, 1957]. Gener-

ally, the best results were provided by equations involving the basin magnitude, the ruggedness number, and the first-order stream frequency. For watersheds having low flash flood potential (Indiana and the Appalachian Plateau), morphometric parameters were better estimators of the mean annual flood ($Q_{0.5}$) than the maximum discharge of record (Q_{max}). This again suggests that drainage networks adjust to and reflect the magnitude and frequency of the dominant runoff events, which in turn reflect the intensity, duration, areal extent, and frequency of the rainfall inputs. Although this morphometric adjustment is probably to a range of discharges, the values of Q_{max} and $Q_{0.5}$ can be thought of as end members of the discharge spectrum.

DISCUSSION

Several general trends are apparent from the morphometric data. With the exception of central Texas, basin relief is higher for the flash flood prone regions than for the low-potential regions. Furthermore the north central Utah and southern California drainage basins have the highest drainage density values. High basin relief combined with high drainage density creates steep short hillslopes, minimizing the length of overland flow and again more rapidly concentrating runoff. Central Texas has intermediate values of basin relief and drainage density but perhaps the greatest flood discharges. The coarser drainage texture and lower basin relief is probably offset by the more extreme rainfall events and the thin impervious lithosols developed on the Edwards Plateau. In contrast, the

TABLE 7. Correlation Matrix of Morphometric Data and Runoff Data for Central Texas

	Drainage Area	Strahler Order	Shreve Magnitude	Relief	Basin Length	Ruggedness	Relief Ratio	Drainage Density	First Order Channel Frequency	Maximum Discharge
Drainage area	1.0000									
Strahler order	0.4334	1.0000								
Shreve magnitude	0.3442	0.8647	1.0000							
Relief	0.4539	0.6729	0.6821	1.0000						
Basin length	0.8934	0.3606	0.3078	0.3852	1.0000					
Ruggedness	0.1371	0.7682	0.8494	0.8841	0.0947	1.0000				
Relief ratio	−0.0659	0.5037	0.5451	0.8256	−0.2019	0.8853	1.0000			
Drainage density	−0.3872	0.5637	0.7163	0.3415	−0.3683	0.7401	0.5980	1.0000		
First-order channel frequency	−0.3934	0.5302	0.7278	0.3349	−0.3533	0.7306	0.5817	0.9844	1.0000	
Maximum discharge	0.8320	0.3788	0.2790	0.6328	0.6676	0.3052	0.2643	−0.2911	−0.3343	1.0000

The transform $X \rightarrow \log_{10} X$ was performed.

TABLE 8. Correlation Matrix of Morphometric Data and Runoff Data for North Central Utah

	Drainage Area	Strahler Order	Shreve Magnitude	Relief	Basin Length	Ruggedness	Relief Ratio	Drainage Density	First-Order Channel Frequency	$Q_{0.5}$	$Q_{0.1}$	$Q_{0.01}$	Q_{max}
Drainage area	1.0000												
Strahler order	0.7867	1.0000											
Shreve magnitude	0.9890	0.8008	1.0000										
Relief	-0.1770	0.1218	-0.1125	1.0000									
Basin length	0.9516	0.6654	0.9209	-0.1499	1.0000								
Ruggedness	0.1402	0.4776	0.2310	0.8771	0.0909	1.0000							
Relief ratio	-0.9079	-0.5522	-0.8599	0.4757	-0.9405	0.2177	1.0000						
Drainage density	0.4955	0.7184	0.5905	0.4404	0.3781	0.8141	-0.1897	1.0000					
First-order channel frequency	0.4470	0.4893	0.5746	0.2992	0.3031	0.6205	-0.1761	0.8283	1.0000				
$Q_{0.5}$	0.7326	0.7830	0.7308	-0.0053	0.5732	0.2693	-0.5103	0.5036	0.3655	1.0000			
$Q_{0.1}$	0.6971	0.7795	0.6960	-0.0207	0.5312	0.2462	-0.4794	0.4772	0.3515	0.9924	1.0000		
$Q_{0.01}$	0.6136	0.7531	0.6142	-0.0302	0.4384	0.2166	-0.4017	0.4283	0.3183	0.9579	0.9856	1.0000	
Q_{max}	0.8182	0.8780	0.8207	0.0379	0.6792	0.3330	-0.5921	0.5792	0.4354	0.9562	0.9608	0.9336	1.0000

The transform $X \rightarrow \log_{10} X$ was performed.

TABLE 9. Correlation Matrix of Morphometric Data and Runoff Data for San Dimas Experimental Forest, Southern California

	Drainage Area	Strahler Order	Shreve Magnitude	Relief	Basin Length	Ruggedness	Relief Ratio	Drainage Density	First-Order Channel Frequency	$Q_{0.5}$	$Q_{0.1}$	$Q_{0.01}$	Q_{max}
Drainage area	1.0000												
Strahler order	0.6998	1.0000											
Shreve magnitude	0.9406	0.8809	1.0000										
Relief	0.9397	0.6046	0.8471	1.0000									
Basin length	0.9968	0.6633	0.9211	0.9440	1.0000								
Ruggedness	0.8799	0.8684	0.9309	0.8829	0.8657	1.0000							
Relief ratio	-0.8634	-0.5870	-0.8236	-0.6519	-0.8653	-0.6408	1.0000						
Drainage density	-0.0768	0.5825	0.2186	-0.1933	-0.1153	0.2899	-0.0099	1.0000					
First-order channel frequency	-0.5491	0.1639	-0.2327	-0.6064	-0.5878	-0.2287	0.4458	0.7583	1.0000				
$Q_{0.5}$	0.8929	0.5607	0.8125	0.8425	0.8816	0.7156	-0.7497	-0.2220	-0.5575	1.0000			
$Q_{0.1}$	0.9516	0.6843	0.9308	0.8507	0.9369	0.7925	-0.8625	-0.0780	-0.4345	0.9049	1.0000		
$Q_{0.01}$	0.7947	0.7832	0.8920	0.6651	0.7798	0.8082	-0.7779	0.3327	-0.0805	0.5681	0.8358	1.0000	
Q_{max}	0.9128	0.5814	0.8615	0.8554	0.9010	0.7616	-0.7765	-0.1522	-0.4943	0.8845	0.9559	0.7659	1.0000

The transform $X \rightarrow \log_{10} X$ was performed.

TABLE 10. Correlation Matrix of Morphometric Data and Runoff Data for Indiana Drainage Basins

	Drainage Area	Strahler Order	Shreve Magnitude	Relief	Basin Length	Rugged-ness	Relief Ratio	Drainage Density	First-Order Channel Frequency	$Q_{0.5}$	$Q_{0.1}$	$Q_{0.01}$	Q_{max}
Drainage area	1.0000												
Strahler order	0.7632	1.0000											
Shreve magnitude	0.8396	0.6957	1.0000										
Relief	0.0007	-0.0199	0.2809	1.0000									
Basin length	0.9794	0.7170	0.8102	0.0024	1.0000								
Ruggedness	-0.2167	-0.1105	0.2149	0.9235	-0.2138	1.0000							
Relief ratio	-0.7322	-0.5484	-0.4224	0.6619	-0.7477	0.7702	1.0000						
Drainage density	-0.4643	-0.2041	0.0644	0.5714	-0.4599	0.8425	0.7176	1.0000					
First-order channel frequency	-0.4714	-0.2709	0.0832	0.4548	-0.4814	0.7465	0.6574	0.9564	1.0000				
$Q_{0.5}$	0.3731	0.4148	0.6695	0.6413	0.3537	0.6409	0.1530	0.4710	0.4025	1.0000			
$Q_{0.1}$	0.2740	0.3240	0.6296	0.6499	0.2476	0.6940	0.2387	0.5717	0.5195	0.9855	1.0000		
$Q_{0.01}$	0.1881	0.2485	0.5848	0.6407	0.1554	0.7206	0.3023	0.6411	0.6044	0.9530	0.9906	1.0000	
Q_{max}	0.1784	0.1795	0.5405	0.6648	0.1601	0.7112	0.3137	0.5867	0.5503	0.9611	0.9865	0.9854	1.0000

The transform $X \rightarrow \log_{10} X$ was performed.

TABLE 11. Correlation Matrix of Morphometric Data and Runoff Data for the Appalachian Plateau Drainage Basins

	Drainage Area	Strahler Order	Shreve Magnitude	Relief	Basin Length	Rugged-ness	Relief Ratio	Drainage Density	First-Order Channel Frequency	$Q_{0.5}$	$Q_{0.1}$	$Q_{0.01}$	Q_{max}
Drainage area	1.0000												
Strahler order	0.8889	1.0000											
Shreve magnitude	0.9711	0.9241	1.0000										
Relief	0.6553	0.3589	0.5281	1.0000									
Basin length	0.9308	0.8797	0.8782	0.6038	1.0000								
Ruggedness	0.6320	0.4663	0.5454	0.9187	0.5736	1.0000							
Relief ratio	-0.8114	-0.8598	-0.7972	-0.2369	-0.8875	-0.2450	1.0000						
Drainage density	-0.2469	0.1279	-0.1210	-0.4629	-0.2462	-0.0752	0.0580	1.0000					
First-order channel frequency	-0.7820	-0.5416	-0.6112	-0.7855	-0.7968	-0.6591	0.6194	0.5095	1.0000				
$Q_{0.5}$	0.9742	0.9024	0.9570	0.6007	0.9401	0.6135	-0.8773	-0.1492	-0.7345	1.0000			
$Q_{0.1}$	0.9742	0.8971	0.9603	0.5967	0.9324	0.6094	-0.8705	-0.1488	-0.7260	0.9979	1.0000		
$Q_{0.01}$	0.9703	0.8863	0.9567	0.5891	0.9255	0.5981	-0.8676	-0.1550	-0.7226	0.9927	0.9983	1.0000	
Q_{max}	0.9497	0.8259	0.9474	0.6254	0.8446	0.6148	-0.7474	-0.2082	-0.6811	0.9418	0.9574	0.9664	1.0000

The transform $X \rightarrow \log_{10} X$ was performed.

TABLE 12. Regression Formulas for Predicting Flood Magnitudes From Drainage Basin Morphometry in Diverse Hydrogeomorphic Regions

Region	Equation	F Ratio	R^2	Probability	Standard Error of Estimate
Central Texas	$Q_{max} = 17369 M^{0.43} H D^{0.54} F_1^{-0.96}$	$(3, 9) = 16.41$	0.85	0.001	0.1000
	$Q_{max} = 36650 M^{0.64} R R^{0.54} D D^{-1.68}$	$(3, 9) = 8.59$	0.74	0.01	0.1295
Southern California	$Q_{max} = 155 M^{1.04} H D^{-0.63} F_1^{-0.73}$	$(3, 8) = 14.87$	0.85	0.001	0.2746
	$Q_{max} = 380 M^{0.89} D D^{-1.87}$	$(2, 9) = 28.56$	0.86	0.0001	0.2450
North central Utah	$Q_{max} = 23 M^{0.90} H D^{1.19} F_1^{-1.58}$	$(3, 7) = 9.13$	0.72	0.005	0.2923
	$Q_{max} = 38618 M^{2.20} R R^{2.61} F_1^{-3.73}$	$(3, 7) = 11.50$	0.83	0.005	0.2286
Indiana	$Q_{max} = 424 M^{0.46} H D^{0.73} F_1^{0.21}$	$(3, 6) = 4.05$	0.67	0.01	0.4200
	$Q_{max} = 424 M^{0.82} R R^{0.67} D D^{0.56}$	$(3, 6) = 3.90$	0.66	0.05	0.4251
	$Q_{0.5} = 115 M^{0.53} H D^{0.62}$	$(2, 7) = 8.46$	0.71	0.025	0.3372
Appalachian Plateau	$Q_{max} = 100 M^{0.79} H D^{0.19} F_1^{-0.29}$	$(3, 7) = 26.14$	0.92	0.0001	0.2153
	$Q_{max} = 38 M^{0.89} D D^{-0.50}$	$(2, 8) = 38.79$	0.91	0.0001	0.2151
	$Q_{0.5} = 5 M^{0.47} H D^{0.61} R R^{-0.73}$	$(3, 7) = 220.94$	0.99	0.0001	0.0818

low-potential flash flood regions have either low (the Appalachian Plateau) or intermediate (Indiana) values of drainage density and low to intermediate basin relief. The combined effect of these two variables will be greater length of overland flow across gently to moderately sloping interfluves, a condition which will result in more attenuated flood hydrographs.

Because relief and drainage density are apparently the two most distinguishing variables, the ruggedness number, the dimensionless product of relief and drainage density, should adequately summarize their interaction. When ruggedness of the study basins is compared to basin magnitude (Figure 7), it is apparent that basins of high flood potential (southern California, north central Utah, and central Texas) have a greater ruggedness at a given basin magnitude than do basins of low flood potential (Indiana and the Appalachian Plateau). Figure 7 effectively summarizes three important variables related to basin response: relief, drainage texture, and drainage network geometry. Because these variables are not well correlated with each other they probably explain different flood-producing components of the drainage basin.

The calculation of a linear distance function (Figure 7) quantifies the break between the two data groups of different flood potential. However, this discriminant function analysis shows that many basins from both high- and low-potential flood regions plot near the boundary separating the two groups. One possible explanation of this grouping is that the permanent morphometric controls are only effective in the determination of flood response for extreme cases of relief and dissection. Thus the California and Utah basins are clearly distinguishable from the Indiana basins by morphometry alone. In these basins the morphology probably enhances the hydrologic response. We suggest that extremely dissected high relief drainage basins may exhibit a high flood potential even given relatively low rainfall inputs (as appears to be the case in Utah). Conversely, low relief poorly dissected basins may have a low flood potential even for high-intensity rainfall. We further suggest that flood potential in basins with intermediate values of dissection and relief (e.g., the Texas and some Appalachian basins) depends to a considerable degree on the nature of the storm input. Although the Texas and Appalachian basins have many morphological similarities, their hydrologic characteristics are greatly different. The high-intensity storms typical of central Texas induce flash floods, whereas the low-intensity storms of the north central Appalachians cause a slower response in basins that are topographically similar to those in Texas.

It is tempting to interpret the relationship illustrated in

Figure 7 in terms of modern geomorphic system concepts [Chorley and Kennedy, 1971]. The complexity in the system is introduced by the great extent to which climate actually controls the basin morphometry. In a region where intense rainfall is an infrequent and random event, as in central Texas, a feedback mechanism enhancing the rapid drainage response can be visualized. The erratically distributed rainfall does not promote vegetation or soil development, and therefore the resulting greater overland flow leads to hillslope rills or gullies (Figure 1), which are eventually incorporated into the channel network. These newly formed first-order channels further increase the response of the drainage system. The reverse would occur in a region where rainfall is temporarily and spatially more uniform. On the Appalachian Plateau, for example, the feedback mechanism would continually work to dampen the basin response by aiding the development of thick soils and dense vegetation, thereby increasing infiltration rates and retarding surface runoff. Regions of intermediate dissection and
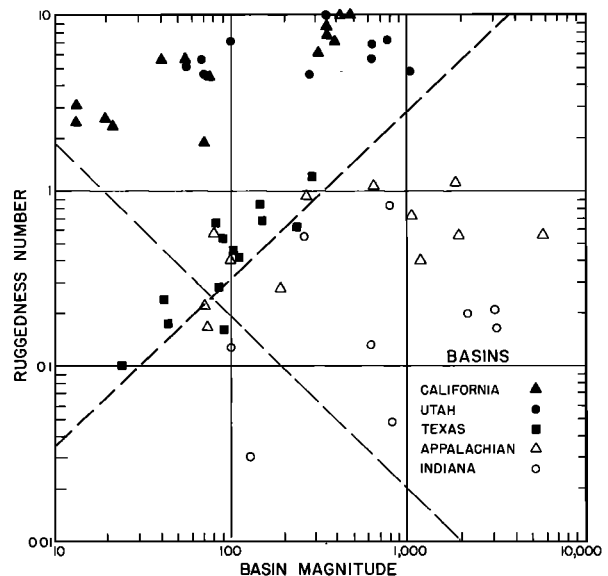

Fig. 7. Ruggedness number (HD) versus basin magnitude (M) for drainage basins in diverse hydrogeomorphic regions. The dot-dash line depicts the result of a discriminant function analysis which yielded $D = M^{-0.066} H D^{0.072}$ with a Mahalanobis D square of 5.848 and $F(2.54) = 38.08$ at probability $P = 0.0001$. The dashed line is drawn perpendicular to the discriminant line through the discriminant index. It graphically defines the boundary between high-flood potential basins (California, Utah, and Texas) and low-flood potential basins (the Appalachian Plateau and Indiana).

relief (Figure 7) apparently have small basins that are most sensitive to changes in transient, i.e., climatic, controls.

REFERENCES

American Geological Institute, *Glossary of Geology,* American Geological Institute, Washington, D. C., 1972.

Anderson, H. W., Flood frequencies and sedimentation from forest watersheds, *Eos Trans. AGU, 30,* 567–584, 1949.

Baker, V. R., Flood hazards along the Balcones Escarpment in central Texas: Alternative approaches to their recognition, mapping and management, *Bur. Econ. Geol. Univ. Tex. Circ. 75-5,* 1–22, 1975.

Baker, V. R., R. K. Holz, S. D. Hulke, P. C. Patton, and M. M. Penteado, Stream network analysis and geomorphic flood plain mapping from orbital and sub-orbital imagery: Application to flood hazard studies in central Texas, NASA final project report, contract NAS 9-13312, pp. 1–187, Nat. Tech. Inform. Serv., Springfield, Va., 1975.

Beard, L. R., Flood flow frequency techniques, *Rep. CRWW-119,* pp. 1–28, Univ. of Tex. Center for Res. in Water Resour., Austin, 1974.

Beard, L. R., Generalized evaluation of flash-flood potential, *Rep. CRWW-124,* pp. 1–27, Univ. of Tex. Center for Res. in Water Resour., Austin, 1975.

Benson, M. A., Factors influencing the occurrence of floods in a humid region of diverse terrain, *U.S. Geol. Surv. Water Supply Pap. 1580-B,* 1–64, 1962.

Blyth, K., and J. C. Rodda, A stream length study, *Water Resour. Res., 9,* 1454–1461, 1973.

Burkham, D. E., Hydrology of Cornfield Wash area and effects of land-treatment practices, Sandoval County, New Mexico, 1951–60, *U.S. Geol. Surv. Water Supply Pap. 1831,* 1–87, 1966.

Butler, E., and R. E. Marsell, Developing a state water plan, Cloudburst floods in Utah, 1939–69, *U.S. Geol. Surv. Coop. Invest. Rep. 11,* pp. 1–103, Utah Div. of Water Resour., Salt Lake City, 1972.

Carlston, C. W., Drainage density and streamflow, *U.S. Geol. Surv. Prof. Pap. 422C,* 1–8, 1963.

Carlston, C. W., and W. F. Langbein, Rapid approximation of drain-density: Line intersection method, *U.S. Geol. Surv. Water Resour. Div. Bull. 11,* 1960.

Chorley, R. J., Climate and morphometry, *J. Geol., 65,* 628–668, 1957.

Chorley, R. J., and B. A. Kennedy, *Physical Geography: A Systems Approach,* pp. 1–370, Prentice-Hall, Englewood Cliffs, N. J., 1971.

Colwick, A. B., H. H. McGill, and F. P. Erichsen, Severe floods at New Braunfels, Texas, *Amer. Soc. Agr. Eng. Pap. 73-206,* 1–8, 1973.

Eardley, A. J., Geology of north-central Wasatch Mountains, Utah, *Geol. Soc. Amer. Bull., 55,* 819–894, 1944.

Gray, D. M. (Ed.), *Handbook on the Principles of Hydrology,* Water Information Center, Port Washington, N. Y., 1970.

Hack, J. T., Studies of longitudinal stream profiles in Virginia and Maryland, *U.S. Geol. Surv. Prof. Pap. 294-B,* 45–97, 1957.

Hadley, R. F., and S. A. Schumm, Hydrology of the upper Cheyenne River basin, *U.S. Geol. Surv. Water Supply Pap. 1531-B,* 186–198, 1961.

Horton, R. E., Drainage basin characteristics, *Eos Trans. AGU, 13,* 350–361, 1932.

Horton, R. E., Erosional development of streams and their drainage basins: Hydrophysical approach to quantitative morphology, *Geol. Soc. Amer. Bull., 56,* 275–370, 1945.

Krumbein, W. C., and F. A. Graybill, *An Introduction to Statistical Models in Geology,* McGraw-Hill, New York, 1965.

Langbein, W. B., et al., Topographic characteristics of drainage basins, *U.S. Geol. Surv. Water Supply Pap. 968-C,* 125–157, 1947.

Lee, M. T., and J. W. Delleur, A program for estimating runoff from Indiana watersheds, 3, Analysis of geomorphic data and a dynamic contributing area model for runoff estimation, report, pp. 1–92, Purdue Univ. Water Resour. Res. Center, Lafayette, Ind., 1972.

Leopold, L. B., and W. B. Langbein, Association and indeterminacy in geomorphology, in *The Fabric of Geology,* pp. 184–192, Freeman, Cooper, San Francisco, Calif., 1963.

Leopold, L. B., M. G. Wolman, and J. P. Miller, *Fluvial Processes in Geomorphology,* W. H. Freeman, San Francisco, Calif., 1964.

Mark, D. M., Line intersection method for estimating drainage density, *Geology, 2,* 235–237, 1974.

Maxwell, J. C., Quantitative geomorphology of the San Dimas experimental forest, California, *Tech. Rep. 19,* pp. 1–95, Office of Nav. Res., Dep. of Geol., Columbia Univ., New York, 1960.

McCoy, R. M., Rapid measurement of drainage density, *Geol. Soc. Amer. Bull., 82,* 757–762, 1971.

Melton, M. A., An analysis of the relation among elements of climate, surface properties and geomorphology, *Tech. Rep. 11,* 102 pp., Office of Nav. Res., Dep. of Geol., Columbia Univ., New York, 1957.

Morisawa, M. E., Quantitative geomorphology of some watersheds in the Appalachian Plateau, *Geol. Soc. Amer. Bull., 73,* 1025–1046, 1962.

Patton, P. C., and V. R. Baker, Low frequency high magnitude floods and their relation to the morphology of streams in central Texas (abstract), *Geol. Soc. Amer. Abstr. Programs, 7(2),* 224–225, 1975.

Rodda, J. C., The flood hydrograph, in *Water, Earth, and Man,* pp. 405–418, Methuen, London, 1969.

Schumm, S. A., Evolution of drainage systems and slopes in badlands at Perth Amboy, New Jersey, *Geol. Soc. Amer. Bull., 67,* 597–646, 1956.

Sherman, L. K., The relation of hydrographs of runoff to size and character of drainage basins, *Eos Trans. AGU, 13,* 332–339, 1932.

Shreve, R. L., Statistical law of stream numbers, *J. Geol., 74,* 17–37, 1966.

Shreve, R. L., Infinite topologically random channel networks, *J. Geol., 75,* 178–186, 1967.

Smart, J. S., Topological properties of channel networks, *Geol. Soc. Amer. Bull., 80,* 1757–1774, 1969.

Snedecor, G. W., and W. G. Cochran, *Statistical Methods,* Iowa State University Press, Ames, 1967.

Stall, J. B., and Y. S. Fok, Discharge as related to stream system morphology, in *Symposium on River Morphology,* pp. 224–235, International Association of Science and Hydrology, Bern, 1967.

Strahler, A. N., Quantitative analysis of watershed geomorphology, *Eos Trans. AGU, 38,* 913–920, 1957.

Strahler, A. N., Dimensional analysis applied to fluvially eroded land forms, *Geol. Soc. Amer. Bull., 69,* 279–300, 1958.

Tinkler, K. J., Active valley meanders in south-central Texas and their wider implications, *Geol. Soc. Amer. Bull., 82,* 1783–1800, 1971.

Trainer, F. W., Drainage density as an indicator of baseflow in part of the Potomac River, *U.S. Geol. Surv. Prof. Pap. 650C,* 177–183, 1969.

Webster, N., *Webster's Seventh New Collegiate Dictionary,* G. and C. Merriam Company, Springfield, Mass., 1965.

Woolley, R. R., Cloudburst floods in Utah, 1850–1938, *U.S. Geol. Surv. Water Supply Pap. 994,* 1–128, 1946.